Characterization of Human iPSC-RPE on a Prosthetic Bruch's Membrane Manufactured From Silk Fibroin

Chad A. Galloway,[1,2] Sonal Dalvi,[1,2] Audra M. A. Shadforth,[3–5] Shuko Suzuki,[3] Molly Wilson,[6] David Kuai,[6] Ali Hashim,[1,2] Leslie A. MacDonald,[1,2] David M. Gamm,[6–8] Damien G. Harkin,[3–5] and Ruchira Singh[1,2,9,10]

[1]Department of Ophthalmology (Flaum Eye Institute), University of Rochester, Rochester, New York, United States
[2]Department of Biomedical Genetics, University of Rochester, Rochester, New York, United States
[3]Queensland Eye Institute, South Brisbane, Queensland, Australia
[4]School of Biomedical Sciences, Queensland University of Technology, Brisbane, Queensland, Australia
[5]Institute of Health and Biomedical Innovation, Queensland University of Technology, Kelvin Grove, Queensland, Australia
[6]Waisman Center, University of Wisconsin, Madison, Wisconsin, United States
[7]Department of Ophthalmology and Visual Sciences, University of Wisconsin, Madison, Wisconsin, United States
[8]McPherson Eye Research Institute, University of Wisconsin, Madison, Wisconsin, United States
[9]Center for Visual Science, University of Rochester, Rochester, New York, United States
[10]Univeristy of Rochester Stem Cell and Regenerative Medicine Institute, Rochester, New York, United States

Correspondence: Ruchira Singh, Department of Ophthalmology (Flaum Eye Institute), 601 Elmwood Avenue, Box 314, University of Rochester, Rochester, NY 14642, USA; ruchira_singh@urmc.rochester.edu.

CAG and SD contributed equally to the work presented here and should therefore be regarded as equivalent authors.

Submitted: October 15, 2017
Accepted: April 24, 2018

Citation: Galloway CA, Dalvi S, Shadforth AMA, et al. Characterization of human iPSC-RPE on a prosthetic Bruch's membrane manufactured from silk fibroin. *Invest Ophthalmol Vis Sci*. 2018;59:2792–2800. https://doi.org/10.1167/iovs.17-23157

Purpose. RPE cell transplantation as a potential treatment for AMD has been extensively investigated; however, in AMD, ultrastructural damage affects both the RPE and its underlying matrix support, the Bruch's membrane (BrM). An RPE monolayer supported by a surrogate scaffold could thus provide a more effective approach to cell-based therapy for AMD. Toward this goal, we aimed to establish a functional human induced pluripotent stem cell–derived (hiPSC)-RPE monolayer on a *Bombyx mori* silk fibroin (BMSF) scaffold.

Methods. RPE differentiated from five distinct hiPSC lines were cultured on BMSF membrane coated with extracellular matrix (ECM, COL1), and either regular tissue culture plastic or Transwell coated with ECM (LAM-TCP). Morphologic, gene and protein expression, and functional characteristics of the hiPSC-RPE cultured on different membranes were compared in longitudinal experiments spanning 1 day to ≥3 months.

Results. The hiPSC-RPE monolayers on ECM-coated BMSF and TCP could be maintained in culture for ≥3 months and displayed RPE-characteristic morphology, pigmentation, polarity, and expression of RPE signature genes and proteins. Furthermore, hiPSC-RPE on both ECM-coated BMSF and TCP displayed robust expression and secretion of several basement membrane proteins. Importantly, hiPSC-RPE cells on COL1-BMSF and LAM-TCP showed similar efficacy in the phagocytosis and degradation of photoreceptor outer segments.

Conclusions. A biomaterial scaffold manufactured from silk fibroin supports the maturation and long-term survival of a functional hiPSC-RPE monolayer. This has significant implications for both in vitro disease modeling and in vivo cell replacement therapy.

Keywords: Bruch's membrane, BrM, tissue engineering, silk fibroin, human induced pluripotent stem cells, hiPSCs, retinal pigment epithelium, RPE

The Bruch's membrane (BrM) plays an important role in vision by supporting both RPE cell survival and function.[1] For instance, BrM provides the necessary structural support to the overlying RPE layer and acts as a conduit for the diffusion of biomolecules to and from RPE cells.[1] Furthermore, BrM is the primary site of disease pathology in AMD.[2,3] In fact, the structural integrity of BrM is affected before the manifestation of overt clinical symptoms in AMD. The incorporation of a BrM-like structure in the in vitro cell model(s) and in vivo RPE implant(s) would thus offer a more thorough and tractable approach for disease modeling and transplantation efforts focused on AMD. For example, a biocompatible scaffold used as a surrogate to BrM could serve as an ideal cell carrier during implantation, and act as a template to guide reconstruction of the subretinal architecture in situ during late-stage AMD, when vision is deteriorating and significant ultrastructural damage is likely.

A BrM substitute should ideally mimic the physical and biochemical properties of this structure; however, it also may be designed simply as a template to support RPE cell implantation and subsequent tissue regeneration. In either case, the material used should be thin (3–5 μm), strong enough to support handling during cell culture and implantation, sufficiently permeable to allow movement of growth factors and waste products, and biologically inert. Although numerous studies have evaluated potential biomaterial scaffolds (extensively tabulated by Jha and Bharti[4]), few have addressed the specific requirements of a BrM surrogate. One of these biomaterials, a permeable polyester substrate (Clinical Trial #NCT01691261) has been transplanted into a human patient;

however, the trial is currently suspended. Another clinical trial (Clinical Trial #NCT02590692), using a synthetic parylene scaffold, is currently under way.[5]

In the absence of a clear material of choice for constructing a synthetic BrM or template, our group has focused its attention on assessing the potential of the silk structural protein fibroin and especially that isolated from cocoons of the domesticated silkworm *Bombyx mori*.[6–10] There are several properties of *Bombyx mori* silk fibroin (BMSF) that make it a viable candidate for study. Isolated fibroin protein, when dissolved in an aqueous solution and cast as a film and dried, results in a transparent membrane that is strong, flexible, and customizable for required thickness (3 μm),[8] permeability, and ECM inclusions.[7] Although a similar thickness to the native BrM, BMSF-derived membranes have been shown to demonstrate increased permeability to dextran compared with native aged BrM.[7] Importantly, BMSF membranes, as used in this study, have a similar modulus of elasticity to that of BrM-choroid isolations.[8,11] Furthermore, as a protein, BMSF is less likely to yield toxic degradation products in vivo and is readily amenable to surface modifications aimed at optimization of cell attachment and growth.[8,9] Moreover, BMSF can be readily isolated and fashioned into a variety of different structures, including membranes and sponges, using relatively inexpensive techniques and without need for toxic chemicals.[10] For example, aqueous solutions of hydrolyzed BMSF form transparent membranes of varying thickness according to the volume of solution applied.

The biocompatibility and tensile strength of fibroin silk has in fact led to its use in diverse applications such as investigation of its utility in vascular grafts[12] and as a component of anterior cruciate ligament surrogates (SeriACL), currently in a clinical trial (NCT00490594). The biocompatibility of BMSF within the ocular tissue has also been investigated and is supported by the absence of an inflammatory response or neovascularization when implanted into the corneal stroma of rabbits for a period of up to 6 months[13,14] and in the subretinal space in the Royal College of Surgeons (RCS) rat model of retinitis pigmentosa for 10 months.[15] With regard to the suitability of BMSF scaffold to support RPE growth, we previously demonstrated the growth of RPE cells isolated from cadaveric tissue, as well as the ARPE-19 cell line on BMSF membranes measuring between 3 and 5 μm in thickness.[6–8] Significantly, these BMSF membranes are similar in mechanical properties to BrM,[1,8] and support the diffusion of both pigment epithelium–derived growth factor (PEDF) and VEGF.[6] Nevertheless, given the limitations associated with use of cadaveric RPE cells and the ARPE-19 cell line, a rigorous evaluation of BMSF membrane suitability is now required using a more clinically relevant model, such as RPE derived from human induced pluripotent stem cells (hiPSC-RPE). The aim of the present study, therefore, was to evaluate the function of hiPSC-RPE cells grown on BMSF membrane, a crucial hurdle in promoting this scaffold toward utility for in vitro modeling and the likelihood of its utility in personalized medicine.

Methods

Ethics

Collection of patient samples and subsequent experimental analyses were performed in accordance with Institutional Regulatory Board of the University of Rochester approval (RSRB00056538) and conformed to the requirements of the National Institutes of Health and Declaration of Helsinki.

Generation, Culture, and Maintenance of hiPSCs

hiPSC lines from five distinct individuals were generated using a previously described protocol.[16] All hiPSC lines were characterized for pluripotency before routine culture and differentiation. Pluripotency characterization of four lines has previously been published,[17,18] and characterization of the fifth hiPSC line is shown in Supplementary Figure S1. hiPSC lines were maintained on either irradiated mouse embryonic fibroblasts or Matrigel (Corning, Corning, NY, USA) and were differentiated to RPE in accordance with our previously described protocol.[19–22]

Manufacture and Use of BMSF Membranes

The production of aqueous solutions of fibroin[23] and the preparation of fibroin membranes[7,8] have been previously described in detail by our group. Here, fibroin was used as a coating on tissue culture plastic (TCP) and as a freestanding membrane (~3 μm in thickness) suspended within custom-designed Teflon chambers.[6–8] Fibroin membranes were used with and without a type I collagen (COL1) (Nitta Gelatin, Inc., Osaka, Japan) coating. Laminin- (LAM; Invitrogen, Carlsbad, CA, USA) coated TCP, or LAM-coated polyethylene terephthalate (PET) Transwell inserts (0.4 μm pore size, 10 μm in thickness) (Costar; Corning) were used as the control substrate in individual experiments. A schematic of the various configurations for hiPSC-RPE cell growth used in this study is shown in Supplementary Figure S2.

Differentiation, Passaging, and Culturing RPE on BMSF Membrane

The procedure for inducing hiPSCs toward a retinal fate was performed as previously described.[19,21] Briefly, RPE arose as adherent colonies by day 40 (D40) of hiPSC differentiation. Patches of pure hiPSC-RPE monolayer were dissected from the pigmented (~D60–D90) mixed differentiating culture, passaged with trypsin-EDTA (0.05%) (Thermo Fisher Scientific, Waltham, MA, USA) and plated in retinal differentiation medium (RDM) + 10% fetal bovine serum (FBS) on LAM-coated (4–24 hours) TCP. These cells were designated as passage 1 (P1). After 2 days, the growth media was changed to RDM + 2% FBS and once at confluence, the media was switched to RDM only. Mature monolayers of pure hiPSC-RPE culture at P1 were subsequently dissociated[20] or plated as spherical aggregates[24] (RPE spheres) on BMSF-TCP, COL1-BMSF-TCP and/or on LAM-TCP (Supplementary Fig. S2) and grown to maturity (>D60). In a subset of experiments, hiPSC-RPEs were cultured as polarized monolayers on fibroin membranes (with or without COL1 coating) suspended in specially designed Teflon chambers (Supplementary Fig. S2).[6–8] hiPSC-RPE cells grown on LAM-coated Transwell inserts (Costar) were used as controls in these experiments (Supplementary Fig. S2). Cultures were allowed to mature for at least 90 days before use in experiments.

ECM Isolation

Cells were removed nonenzymatically and the ECM was harvested by incubation in ECM isolation buffer (10 mM Tris pH 6.8, 10% glycerol, and 1% SDS) containing protease inhibitor cocktail (Sigma-Aldrich Corp., St. Louis, MO, USA) at 37°C for 30 minutes, as previously described.[17]

Western Blotting

Total cell lysate and ECM were isolated and resolved by SDS-PAGE in 4% to 20% gels as previously described.[17] Resolved

Investigative Ophthalmology & Visual Science

gels were transferred to polyvinylidene difluoride membranes (Bio-Rad, Hercules, CA, USA) and probed with the following primary antibodies: ACTN (1:750; Santa Cruz Biotechnology, Dallas, TX, USA), BEST1 (1:500; Millipore, Billerica, MA, USA), COL4 (1:1000; Abcam, Cambridge, MA, USA), CRALBP (1:10000),[25] EZR (1:1000, Cell Signaling Technology, Danvers, MA, USA), LAM (1:1000; Abcam), OCLN (1:1000; Thermo Fisher Scientific), RPE65 (1:500; Millipore), RHO (1:500; Millipore), and TIMP3 (1:250; Abcam). Secondary antibodies were host-specific near-infrared (1:12,500) (LiCor, Lincoln, NE, USA) or horseradish peroxidase conjugated (1:10,000) (Jackson ImmunoResearch, West Grove, PA, USA) and signals were detected on the LiCor Odyssey or the Azure C500 (Azure Biosystems, Dublin, CA, USA) imaging systems. After image acquisition, Western blot data were analyzed quantitatively using LiCor Odyssey 3.0 and/or Image Studio Lite version 5.2 (LiCor) and Microsoft Excel (Redmond, WA, USA).

Immunocytochemistry

Mature iPSC-RPE cultures on LAM-TCP or COL1-BMSF in 24 wells, Transwells, and custom-made chambers (described above) were fixed with cold 4% paraformaldehyde for 30 minutes. For whole-mount staining of RPE monolayers, cells were washed with 1X PBS, permeabilized, and blocked in 1X PBS containing 10% normal donkey serum (NDS) (ImmunoReagents, Raleigh, NC, USA) and 0.1% Triton X-100 for 1 hour at room temperature. Incubation in primary antibody was overnight at 4°C in 5% NDS and 0.05% Triton X-100 with the following antibodies: BEST1 (1:50), EZR (1:100), MITF (1:50; Santa Cruz Biotechnology), and ZO-1 (1:100; Invitrogen). For sectioning, paraffin-embedded samples were sectioned at 14 μm before immunofluorescent analyses, and antigen retrieval was conducted as previously described.[17] Processing through primary antibody was the same as whole-mount staining with the following primary antibody concentrations: COL4 (1:100; Abcam), EFEMP1 (1:200; Abcam), TIMP3 (1:50; Abcam and GeneTex, Irvine, CA, USA), and LAM (1:200; Abcam). Host-specific Alexa-Fluor conjugated secondary antibodies were used at 1:500 and samples were coverslipped with Prolong Gold anti-fade reagent (Invitrogen). Immunocytochemical staining was analyzed and images were taken on an LSM 510 META confocal microscope with ZEN 2009 software (Zeiss, Thornwood, NY, USA) for image capture.

Quantitative Real-Time RT-PCR

RNA was isolated using our previously published protocol[17] and in accordance with the manufacturer's instructions. Total RNA was subjected to DNASE1 treatment before cDNA synthesis, which was performed in accordance with the manufacturer's recommendation. Quantitative PCR (qPCR) using gene-specific primers for RPE markers[21] and basement membrane genes (listed in Supplementary Table S1) used SYBR green master mix (Bio-Rad) and was performed in a CFX Bio-Rad thermocycler and analyzed using Bio-Rad CFX Manager V3.1 (Bio-Rad).

Gel Electrophoresis

qPCR products were resolved on 1% agarose gels in 1X TAE buffer (Tris base, acetic acid, and EDTA; Invitrogen) with 0.025% ethidium bromide. DNA was visualized by UV lamp and imaged using the ChemiDoc XRS system (Bio-Rad) and Quantity One software (Bio-Rad).

Experimental Set-Up and Data Analyses

All experiments were performed at least in triplicate on parallel, age-matched (days in culture) hiPSC-RPE cells grown on BMSF versus COL1-BMSF versus LAM-TCP similar tissue culture support (24-well plate versus Transwells and custom-made chambers). Furthermore, data from hiPSC-RPE derived from at least three, but up to five distinct hiPSC lines was used in each individual assay. For quantitative analyses, data are expressed as mean ± SEM throughout the article. Significance was assessed using a two-tailed Student's *t*-test analysis with a cutoff of $P < 0.05$. For simplicity, the terminology LAM-TCP is used to refer to both nonpermeable plastic support and PET Transwells throughout the article.

Results

Long-term Cultures of hiPSC-RPE Are Sustainable on ECM-Coated BMSF

Previous studies using hiPSC-RPE cultures have shown that ECM (LAM)-coated TCP can support hiPSC-RPE cultures for ≥D90.[17,20] Therefore, to compare the viability and maintenance of hiPSC-RPE monolayers on BMSF, we used LAM-coated TCP (LAM-TCP) as the reference standard. Of note, because the ECM substrate used on BMSF was type I collagen (COL1) coating, we confirmed the ability of COL1-coated TCP (COL1-TCP) to sustain long-term RPE cultures like LAM-TCP (data not shown). The seeding of dissociated hiPSC-RPE cells[20] as well as RPE spheres[24] on three different substrates, uncoated BMSF (BMSF), COL1-coated BMSF (COL1-BMSF), and LAM-TCP, in parallel experiments, demonstrated that hiPSC-RPE can adhere, spread, and consequently form a monolayer on BMSF, COL1-BMSF, and LAM-TCP in short-term (14 days) cultures (Fig. 1A, Supplementary Fig. S3A). Interestingly by D40 in culture, contraction of hiPSC-RPE plated on BMSF was observed (Fig. 1A, Supplementary Fig. S3A). In contrast, COL1 coating reduced the observed RPE contraction on BMSF membranes after cell plating and hiPSC-RPE monolayers on COL1-BMSF and LAM-TCP continued to show the RPE-characteristic morphology (Fig. 1B, Supplementary Fig. S3B). To dismiss cell line–specific properties for the contraction of hiPSC-RPE on BMSF alone and to further examine ability of COL1-BMSF to inhibit RPE contraction and promote RPE cell growth, hiPSC-RPE from additional hiPSC lines, derived from different subjects, were cultured for ≥60 days. Importantly, all five hiPSC-RPE lines demonstrated a similar, nearly indistinguishable within a line, morphologic presentation on COL1-BMSF and LAM-TCP in long-term cultures (Fig. 1B, Supplementary Fig. S3).

Polarized Monolayers of hiPSC-RPE on COL1-BMSF Display Robust Expression of RPE Signature Genes and Proteins

The selective stability of hiPSC-RPE plated on COL1-coated BMSF membrane established that the presence of COL1 was sufficient for long-term culture of hiPSC-RPE monolayers on BMSF. Therefore, we selected the COL1-BMSF configuration for further characterization of the hiPSC-RPE monolayer. Consistent with the formation of a polarized monolayer, hiPSC-RPE cultures on COL1-BMSF and LAM-TCP showed apical versus basolateral localization of EZR and BEST1, respectively (Fig. 2A). In addition, tight junction marker ZO-1 and nuclear-localized RPE protein, MITF, displayed similar immunostaining pattern in COL1-BMSF versus LAM-TCP hiPSC-RPE cultures (Figs. 2B, 2C). Furthermore, in agreement with an RPE-characteristic gene and protein expression profile, hiPSC-RPE

Investigative Ophthalmology & Visual Science

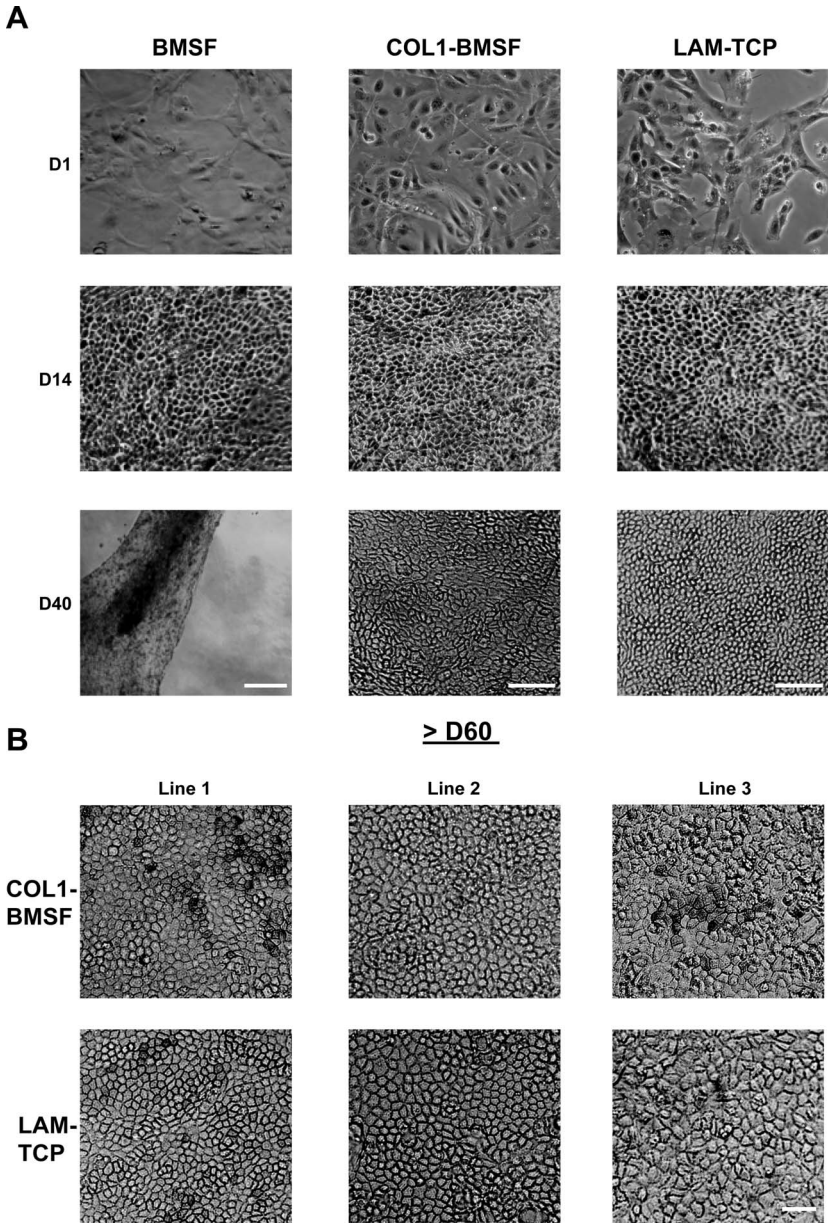

Figure 1. Morphological characterization of hiPSC-RPE cultures on BMSF, COL1-BMSF, and LAM-TCP. (**A**) Light microscopy images of dissociated hiPSC-RPE grown on BMSF membrane alone (BMSF), type I collagen-coated BMSF membrane (COL1-BMSF), or laminin-coated tissue culture plastic (LAM-TCP) at D1, D14, and D40 demonstrated attachment and growth of hiPSC-RPE on all three substrates with characteristic cobblestone morphology. Of note, although hiPSC-RPE grown on COL1-BMSF and LAM-TCP membrane retained characteristic cobblestone morphology at D40, hiPSC-RPE monolayers on BMSF membrane began to selectively retract by D40. *Scale bar*: 250 μm. (**B**) hiPSC-RPE plated on both COL1-BMSF and LAM-TCP remained adherent and had a similar cobblestone morphological appearance in long-term cultures (>D60). *Scale bar*: 50 μm.

culture on COL1-BMSF and LAM-TCP displayed similar and robust expression of RPE signature genes (*BEST1*, *CRALBP*, *MERTK*, *OCLN*, *PEDF*, *MITF*, *RPE65*) and proteins (EZR, BEST1, RPE65, OCLN, CRALBP) (Figs. 2D–F).

hiPSC-RPE Cultured on COL1-BMSF and LAM-TCP Possess a Similar Efficacy in the Phagocytosis and Degradation of Photoreceptor Outer Segments (POS)

The phagocytosis and degradation of POS is a critical function of the RPE cells. To test the competence of hiPSC-RPE cultured on COL1-BMSF versus LAM-TCP to phagocytose and degrade POS, mature monolayers of hiPSC-RPE on COL1-BMSF (Teflon support) or LAM-TCP (Transwells) were incubated apically with 20 POS/RPE cells with unlabeled or labeled POS (FITC-POS) (InVision Bioresources, Seattle, WA, USA). Following a 2-hour incubation, hiPSC-RPE cells were washed extensively to remove any uningested POS from the RPE cell surface. Subsequently, the uptake (0 hour) and degradation (24 hours) of POS by hiPSC-RPE were determined using FITC fluorescence and Western blotting as previously described[20,22] (Fig. 3A). hiPSC-RPE cultured on both COL1-BMSF and LAM-TCP displayed the ability to phagocytose POS (Figs. 3B, 3C). In fact, detecting FITC fluorescence using confocal microscopy

Investigative Ophthalmology & Visual Science

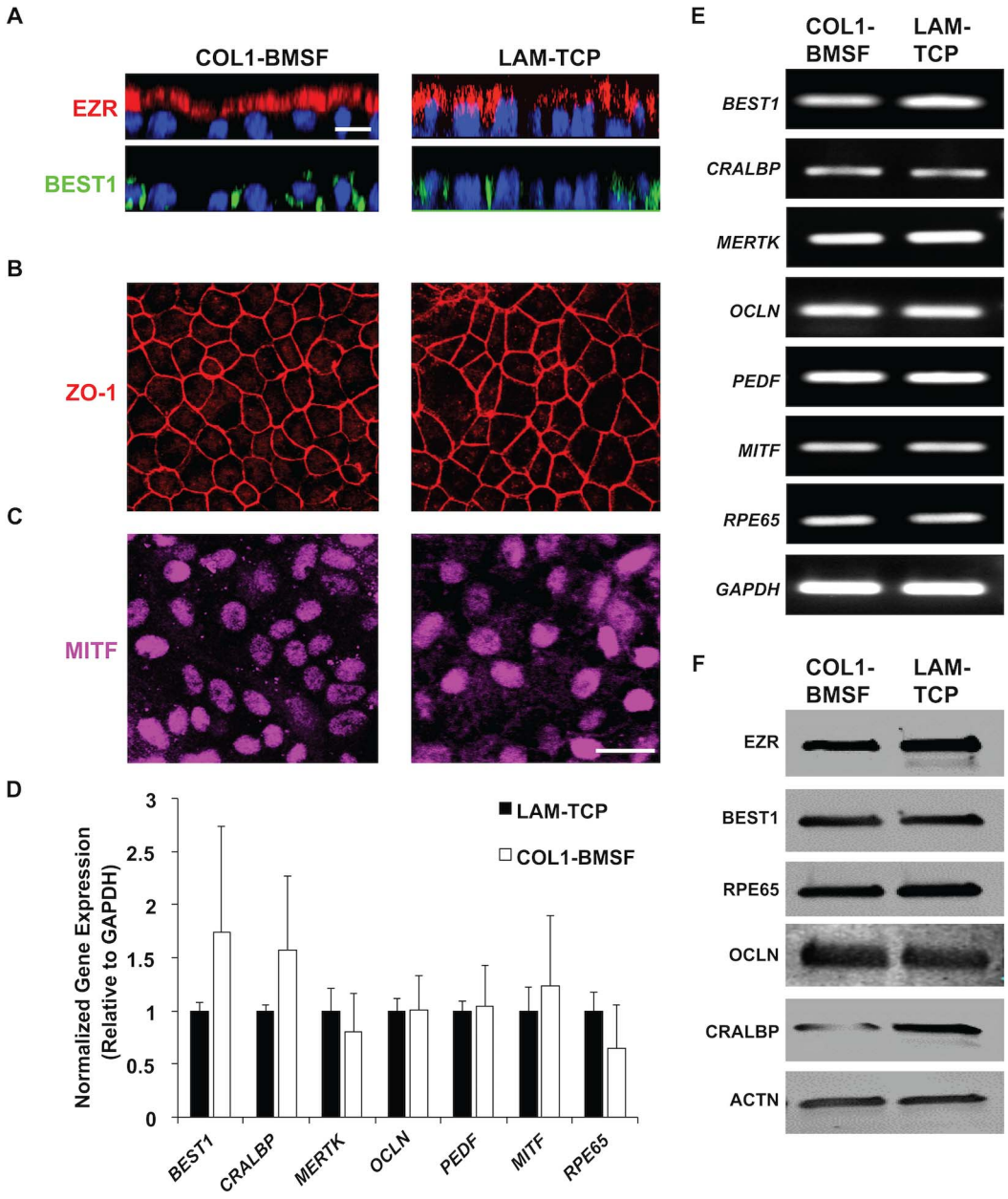

Figure 2. Expression and localization of RPE signature genes and proteins in hiPSC-RPE cultures on COL1-BMSF versus LAM-TCP. (**A–C**) Confocal microscopy revealed the expected (**A**) apical versus basolateral localization of EZR and BEST1, respectively, (**B**) staining of the tight junction marker ZO-1, and (**C**) nuclear presence of MITF in COL1-BMSF and LAM-TCP plated hiPSC-RPE. *Scale bar*: 10 μm. (**D**) qPCR and (**E**) gel electrophoresis analyses showed similar expression of gene-specific PCR product of several RPE-characteristic genes in hiPSC-RPE cultures grown on COL1-BMSF and LAM-TCP. Data are represented as the mean ± SEM. (**F**) Western blot analyses demonstrated similar expression of multiple RPE signature proteins in hiPSC-RPE grown on COL1-BMSF versus LAM-TCP. Note: *GAPDH* and ACTN served as loading controls in qPCR and Western blotting experiments, respectively.

analyses of RPE following FITC-POS incubation, clearly demonstrated the internalization of FITC-POS by hiPSC-RPE cells cultured on both COL1-BMSF and LAM-TCP (Fig. 3B). Similarly, Western blot analyses for Rhodopsin (RHO), a POS-specific protein, at 0- and 24-hour time points demonstrated a robust uptake (0 hour) and subsequent substantial degradation (24 hours) of POS by hiPSC-RPE cultured on both COL1-BMSF and LAM-TCP (Fig. 3C, Supplementary Fig. S4). Overall, although hiPSC-RPE line–specific variability in POS uptake and degradation was seen (Supplementary Fig. S4), the ability of hiPSC-RPE cultures on COL1-BMSF to ingest and digest POS was on par with hiPSC-RPE cultures on LAM-TCP.

hiPSC-RPE Cultured on COL1-BMSF and LAM-TCP Form a Basement Membrane Overlying Their Plating Substrate

In vivo, the BrM is a multilayered physical support for the RPE, composed of basement membranes of the RPE and choroid enveloping the elastin and collagen layers.[1] Although a prosthetic membrane would provide an integral physical support for transplanted RPE, hiPSC-RPE grown on the biomaterial membrane should ideally possess the ability to generate basement membrane endogenously. A recent article has shown that hiPSC-RPEs in culture are capable of forming a

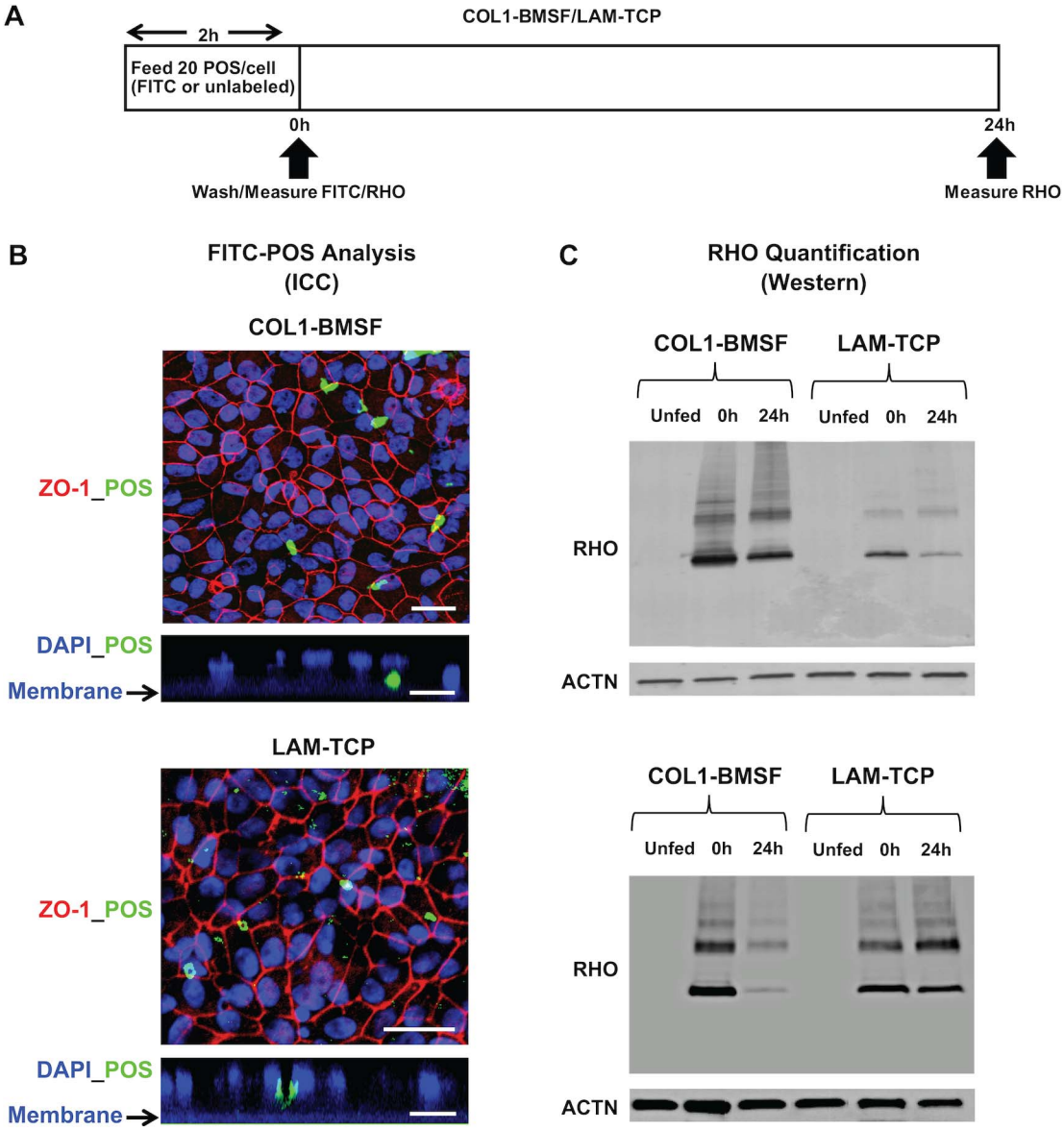

Figure 3. Phagocytosis and degradation of POS by hiPSC-RPE grown on COL1-BMSF versus LAM-TCP. (**A**) A schematic representation of the experimental strategy to assess POS phagocytosis (2 hours post incubation with POS), and degradation (24 hours following incubation with POS). (**B**) Qualitative analyses of POS uptake using magnitude and localization of FITC fluorescence with confocal microscopy demonstrated similar uptake of FITC-labeled POS by hiPSC-RPE cultures on both COL1-BMSF and LAM-TCP. Note: Autofluorescence of the respective membrane (indicated by an *arrow*), COL1-BMSF or LAM-TCP, is beneath the hiPSC-RPE monolayers. *Scale bar*: 20 µm. (**C**) Representative images of a specific Western blot measuring the amount of RHO (a POS-specific protein), in hiPSC-RPE monolayer cell lysate after POS feeding showing similar or better efficiency in POS uptake at the 0-hour time point and POS degradation at the 24-hour time point (relative to the 0-hour uptake) by hiPSC-RPE cultures grown on COL1-BMSF compared with hiPSC-RPE cultures on LAM-TCP. Note: ACTN served as loading control for these experiments, and the quantification of RHO protein levels at the 0 hour and 24 hours is shown in Supplementary Figure S4.

defined basement membrane with proper localization of several RPE-secreted basement membrane proteins.[17] Consistent with these findings, gene expression analyses of hiPSC-RPE grown on COL1-BMSF and LAM-TCP revealed the expression of genes encoding several basement membrane components, including *COL1A1*, *FN1*, *LAMB1*, *LAMB2*, and *LAMC1* (Fig. 4A). Importantly, Western blot and immunocytochemical analyses demonstrated the proper secretion and expected localization of several RPE basement membrane proteins, COL4, EFEMP1, LAM, and TIMP3, in hiPSC-RPE cultures maintained on both COL1-BMSF and LAM-TCP (Figs. 4B–F).

Discussion

In this study, using hiPSC-RPE from five distinct human subjects, we demonstrate the utility of a BMSF membrane to serve as an RPE scaffold in long-term cultures. Specifically, we show that COL1-coated BMSF membrane is sufficient to support a physiologic hiPSC-RPE monolayer with cellular characteristics similar to hiPSC-RPE grown on LAM-TCP with respect to the morphological appearance and pigmentation, the expression and localization of RPE signature genes/proteins, the secretion and localization of basement membrane proteins, and the ability to phagocytose and degrade POS.

Investigative Ophthalmology & Visual Science

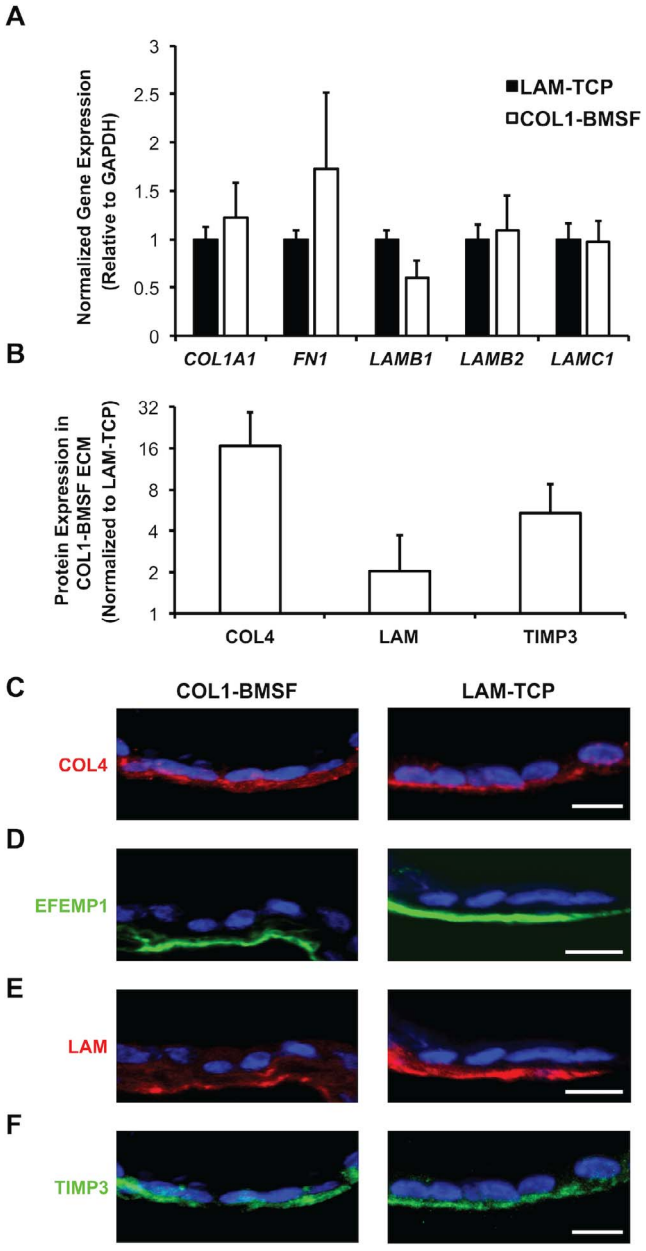

Figure 4. Expression and localization of basement membrane proteins in hiPSC-RPE cultures on COL1-BMSF versus LAM-TCP. (**A**) qPCR analyses revealed similar expression of genes encoding specific basement membrane proteins in hiPSC-RPE monolayers grown on COL1-BMSF and LAM-TCP. *GAPDH* served as loading control for the qPCR analysis. (**B**) Quantitative Western blot analyses of ECM extracts underlying hiPSC-RPE cultures demonstrated equivalent or higher levels of specific basement membrane proteins; COL4, LAM, and TIMP3 in hiPSC-RPE cultures grown on COL1-BMSF. (**C**–**F**) Confocal microscopy of hiPSC-RPE monolayers after immunostaining revealed similar localization of several basement membrane proteins, (**C**) COL4, (**D**) EFEMP1, (**E**) LAM, and (**F**) TIMP3 in hiPSC-RPE cultures grown on both COL1-BMSF and LAM-TCP. *Scale bar*: 10 μm. Data are represented as the mean ± SEM.

Currently, there is no corrective treatment available for a large proportion of patients with AMD, and with an aging population, it is predicted that 288 million people will be afflicted worldwide by 2040.[26] Cell replacement therapies have been explored as a treatment option to repair the damaged subretinal architecture preceding late-stage disease complications, but there are multiple technical challenges to overcome before this therapeutic option becomes viable. The overarching goal of such an intervention is to implant healthy RPE tissue in the retina, thereby preserving the patient's remaining sight by supporting the function of the existing photoreceptor cells. It is reasonable to anticipate that a surgical insertion of a healthy RPE monolayer will require the removal of the host tissue before implantation occurs. Furthermore, it is highly likely that the implanted RPE and its supporting scaffold will need to be semipermanent structures in the patient's subretinal space. A "semipermanent implant strategy" that incorporates both cells and a support scaffold, that is, a patient's own RPE cells (hiPSC-RPE) on a BrM-like scaffold, represents a targeted alternative strategy for RPE-specific cell replacement in AMD.

The BrM in vivo is a multilayered physical support for the RPE, composed of basement membranes of the RPE and choroid sandwiching the elastin and collagen layers.[1] Importantly, a synergistic effort between RPE and the choriocapillaris (CC) in vivo is responsible for BrM development[27] and the ECM protein constituents of BrM are synthesized partially by both RPE cells and CC.[27] Thus, one approach to making a physiological BrM-like ECM would be to co-culture RPE cells and choroidal endothelial cells, both of which have previously been generated from hiPSCs.[20,28,29] However, it is plausible that to generate the BrM, the temporal execution of in vivo development, in which the RPE monolayer development and maturation precedes that of CC development,[30] will need to be mimicked to engineer such a model. Furthermore, it is also likely that apart from choroidal endothelial cells, other cell types present in the choroid (e.g., pericytes) would need to be incorporated into such a cellular model for the development of a biological BrM.[31] Given that much of the comprehensive choroid physiology is unknown, this may be a daunting task. An alternative approach to autonomous generation of a BrM-like support for RPE is the development of synthetic material (e.g., BMSF, as used in this study) with physical characteristics similar to the human BrM in vivo. Importantly, a bioengineered scaffold like BMSF membrane, as demonstrated in this study, will need to be optimized (e.g., via COL1 coating) to support long-term culture of RPE cells. Furthermore, aside from supporting long-term RPE cultures, a critical quality of a bioscaffold, like BMSF, for disease modeling and implantation studies would be its ability to support key RPE cell functions. For instance, the inability to efficiently process POS has been implicated in multiple maculopathies, including AMD[21,32,33]; therefore, any viable RPE scaffold option for disease modeling or cellular replacement with respect to AMD must not interfere with the ability of RPE cells to phagocytose and degrade POS. It is noteworthy that the ability for hiPSC-RPE grown on COL1-coated BMSF to ingest and degrade POS was similar to hiPSC-RPE on well-characterized ECM substrates.[20–22] Of note, although promising, our current studies do not evaluate the biocompatibility of BMSF in supporting hiPSC-RPE implant in vivo. Therefore, future animal model studies determining the safety and impact of hiPSC-RPE-BMSF implant on retinal function and integrity in the long-term, including in vivo assessment of RPE cell function, will be important to ultimately validate BMSF scaffold for cell-based therapy.

With regard to the usage of BMSF implant in vivo and in particular with reference to the eye, it is noteworthy that (1) corneal epithelial cell grafts on silk fibroin are stable for up to 6 months in a rabbit model,[13,14,34] and (2) a photovoltaic implant supported by BMSF in the subretinal space of the RCS rat model had no adverse immune reactivity for up to 10 months.[15] Although supportive of the biocompatibility and

utility of the BMSF scaffold in the subretinal space, the RCS rat of retinitis pigmentosa is not an appropriate model for AMD. Furthermore, and relevant to the eye, silk fibroin has previously been shown to promote angiogenesis.[35] There are also studies in which BMSF has been implanted into naturally vascularized tissues, such as the dermis, and has then been followed for evidence of vascular in-growth.[36] However, there are distinct differences in the nature of these studies, primarily involving the silk fibroin preparation. For instance, although we have cast fibroin membranes to the thickness of the BrM 3 μm ± 1 μm, the angiogenesis study[35] sonicated the fibroin preparations to create a three-dimensional soft tissue for integration of cells into in the matrix. Given the nature of the experimental set-up, it is not clear whether in vivo cells would integrate in these scaffolds, as the premixed cells do in vitro. Importantly and highlighting a nonvascular response of BMSF implant in the eye, a recent study using a silk fibroin scaffold in the subretinal space of the RCS rat model did not report choroidal neovascularization promotion.[15] However, as mentioned previously, given the difference in the RCS rat model disease pathology and AMD, the next logical step would be the utilization of BMSF scaffold in an appropriate animal model. To evaluate the grafting of an hiPSC-RPE-BMSF complex as a possible approach for disease modeling or cell replacement therapy for AMD, an animal model should present with RPE dystrophy, ideally with minimal impact to the photoreceptor cells, as these would be characteristics of the AMD retina before the irreversible loss of photoreceptors. Few murine models for geographic atrophy AMD exist, but they include an RPE DICER knockout model[37] and a chemically induced RPE ablation model.[38] Although the former has a total loss of RPE and photoreceptors at all time points reported, the latter demonstrated RPE ablation within 7 days of intraocular sodium iodate injection, which was recovered using hiPSC-RPE transplantation.[38] Although RPE cell death after sodium iodate injection was complete within 3 days, it preceded photoreceptor death, which was not complete, allowing a window of grafting. Larger-eyed animals, such as rabbits, also have been used successfully for similar implantation studies with parylene scaffolds,[39] and may alleviate technical challenges of the implantation surgery. Ultimately, more advanced models, such as nonhuman primates, which have now been reported to be amendable to hiPSC-RPE transplantation in major histocompatibility complex–matched RPE allografts,[40] will reveal the true compatibility of such RPE replacement therapies.

Altogether, our data show that long-term maintenance of a functional hiPSC-RPE monolayer is possible on a synthetic biocompatible scaffold, BMSF, which has previously been shown to be biocompatible in vivo and to also possess numerous physical characteristics akin to BrM.[6–10] This has significant implications for both in vitro (e.g., disease modeling, drug screening) as well as in vivo (cell replacement) applications using hiPSC-RPE cells.

Acknowledgments

Supported by the Brightfocus Foundation Macular Degeneration Grant (RS), David Bryant Trust (RS), Foundation of Fighting Blindness Individual Investigator Award (RS), Knights Templar Eye Foundation (RS), National Institutes of Health NIH-1R01EY028167 (RS), Retina Research Foundation and Research to Prevent Blindness, Research to Prevent Blindness Career Development Award (RS), Unrestricted Challenge Grant to Department of Ophthalmology at University of Rochester and University of Wisconsin-Madison, Retina Research Foundation E. A. Humble Directorship of the McPherson Eye Research Institute (DMG), Sandra Lemke Trout Chair in Eye Research (DMG), and grants awarded by the National Health and Medical Research Council of Australia (DGH, AMAS), the Macular Disease Foundation of Australia (DGH, AMAS), and the Queensland Eye Institute Foundation, Australia (DGH, AMAS, SS).

Disclosure: **C.A. Galloway**, None; **S. Dalvi**, None; **A.M.A. Shadforth**, None; **S. Suzuki**, None; **M. Wilson**, None; **D. Kuai**, None; **A. Hashim**, None; **L.A. MacDonald**, None; **D.M. Gamm**, None; **D.G. Harkin**, None; **R. Singh**, None

References

1. Curcio CA, Johnson M. Structure, function and pathology of Bruch's membrane. In: Ryan SJ, Wilkinson CP, Hinton DR, Sadda S, Wiedmann P, eds. *Retina*. London, UK: Elsevier; 2013:466–481.
2. Green WR. Histopathology of age-related macular degeneration. *Mol Vis*. 1999;5:27.
3. Capon MR, Marshall J, Krafft JI, Alexander RA, Hiscott PS, Bird AC. Sorsby's fundus dystrophy. A light and electron microscopic study. *Ophthalmology*. 1989;96:1769–1777.
4. Jha BS, Bharti K. Regenerating retinal pigment epithelial cells to cure blindness: a road toward personalized artificial tissue. *Curr Stem Cell Rep*. 2015;1:79–91.
5. Lu B, Zhu D, Hinton D, Humayun MS, Tai YC. Mesh-supported submicron parylene-C membranes for culturing retinal pigment epithelial cells. *Biomed Microdevices*. 2012;14:659–667.
6. Shadforth AMA, Suzuki S, Theodoropoulos C, Richardson NA, Chirila TV, Harkin DG. A Bruch's membrane substitute fabricated from silk fibroin supports the function of retinal pigment epithelial cells in vitro. *J Tissue Eng Regen Med*. 2017;11:1915–1924.
7. Shadforth AM, George KA, Kwan AS, Chirila TV, Harkin DG. The cultivation of human retinal pigment epithelial cells on Bombyx mori silk fibroin. *Biomaterials*. 2012;33:4110–4117.
8. Shadforth AM, Suzuki S, Alzonne R, et al. Incorporation of human recombinant tropoelastin into silk fibroin membranes with the view to repairing Bruch's membrane. *J Funct Biomater*. 2015;6:946–962.
9. Suzuki S, Dawson RA, Chirila TV, et al. Treatment of silk fibroin with poly(ethylene glycol) for the enhancement of corneal epithelial cell growth. *J Funct Biomater*. 2015;6:345–366.
10. Harkin DG, George KA, Madden PW, Schwab IR, Hutmacher DW, Chirila TV. Silk fibroin in ocular tissue reconstruction. *Biomaterials*. 2011;32:2445–2458.
11. Chan WH, Hussain AA, Marshall J. Youngs modulus of Bruchs membrane: implications for AMD. *Invest Ophthalmol Vis Sci*. 2007;48:2187–2187.
12. Enomoto S, Sumi M, Kajimoto K, et al. Long-term patency of small-diameter vascular graft made from fibroin, a silk-based biodegradable material. *J Vasc Surg*. 2010;51:155–164.
13. Vazquez N, Rodriguez-Barrientos CA, Aznar-Cervantes SD, et al. Silk fibroin films for corneal endothelial regeneration: transplant in a rabbit descemet membrane endothelial keratoplasty. *Invest Ophthalmol Vis Sci*. 2017;58:3357–3365.
14. Higa K, Takeshima N, Moro F, et al. Porous silk fibroin film as a transparent carrier for cultivated corneal epithelial sheets. *J Biomater Sci Polym Ed*. 2011;22:2261–2276.
15. Maya-Vetencourt JF, Ghezzi D, Antognazza MR, et al. A fully organic retinal prosthesis restores vision in a rat model of degenerative blindness. *Nat Mater*. 2017;16:681–689.
16. Okita K, Matsumura Y, Sato Y, et al. A more efficient method to generate integration-free human iPS cells. *Nat Methods*. 2011;8:409–412.

17. Galloway CA, Dalvi S, Hung SSC, et al. Drusen in patient-derived hiPSC-RPE models of macular dystrophies. *Proc Natl Acad Sci U S A*. 2017;114:E8214–E8223.
18. Phillips MJ, Wallace KA, Dickerson SJ, et al. Blood-derived human iPS cells generate optic vesicle-like structures with the capacity to form retinal laminae and develop synapses. *Invest Ophthalmol Vis Sci*. 2012;53:2007–2019.
19. Meyer JS, Shearer RL, Capowski EE, et al. Modeling early retinal development with human embryonic and induced pluripotent stem cells. *Proc Natl Acad Sci U S A*. 2009;106: 16698–16703.
20. Singh R, Phillips MJ, Kuai D, et al. Functional analysis of serially expanded human iPS cell-derived RPE cultures. *Invest Ophthalmol Vis Sci*. 2013;54:6767–6778.
21. Singh R, Shen W, Kuai D, et al. iPS cell modeling of Best disease: insights into the pathophysiology of an inherited macular degeneration. *Hum Mol Genet*. 2013;22:593–607.
22. Singh R, Kuai D, Guziewicz KE, et al. Pharmacological modulation of photoreceptor outer segment degradation in a human iPS cell model of inherited macular degeneration. *Mol Ther*. 2015;23:1700–1711.
23. Chirila T, Barnard Z, Zainuddin, Harkin DG, Schwab IR, Hirst L. *Bombyx mori* silk fibroin membranes as potential substrata for epithelial constructs used in the management of ocular surface disorders. *Tissue Eng Part A*. 2008;14:1203–1211.
24. Gamm DM, Melvan JN, Shearer RL, et al. A novel serum-free method for culturing human prenatal retinal pigment epithelial cells. *Invest Ophthalmol Vis Sci*. 2008;49:788–799.
25. Saari JC, Nawrot M, Stenkamp RE, Teller DC, Garwin GG. Release of 11-cis-retinal from cellular retinaldehyde-binding protein by acidic lipids. *Mol Vis*. 2009;15:844–854.
26. Wong WL, Su X, Li X, et al. Global prevalence of age-related macular degeneration and disease burden projection for 2020 and 2040: a systematic review and meta-analysis. *Lancet Glob Health*. 2014;2:e106–e116.
27. Booij JC, Baas DC, Beisekeeva J, Gorgels TG, Bergen AA. The dynamic nature of Bruch's membrane. *Prog Retin Eye Res*. 2010;29:1–18.
28. Belair DG, Whisler JA, Valdez J, et al. Human vascular tissue models formed from human induced pluripotent stem cell derived endothelial cells. *Stem Cell Rev*. 2015;11:511–525.
29. Zanotelli MR, Ardalani H, Zhang J, et al. Stable engineered vascular networks from human induced pluripotent stem cell-derived endothelial cells cultured in synthetic hydrogels. *Acta Biomater*. 2016;35:32–41.
30. Hasegawa T, McLeod DS, Bhutto IA, et al. The embryonic human choriocapillaris develops by hemo-vasculogenesis. *Dev Dyn*. 2007;236:2089–2100.
31. Kur J, Newman EA, Chan-Ling T. Cellular and physiological mechanisms underlying blood flow regulation in the retina and choroid in health and disease. *Prog Retin Eye Res*. 2012; 31:377–406.
32. Sparrow JR, Boulton M. RPE lipofuscin and its role in retinal pathobiology. *Exp Eye Res*. 2005;80:595–606.
33. Winkler BS, Boulton ME, Gottsch JD, Sternberg P. Oxidative damage and age-related macular degeneration. *Mol Vis* 1999; 5:32.
34. Hazra S, Nandi S, Naskar D, et al. Non-mulberry Silk fibroin biomaterial for corneal regeneration. *Sci Rep*. 2016;6:21840.
35. Sun W, Motta A, Shi Y, et al. Co-culture of outgrowth endothelial cells with human mesenchymal stem cells in silk fibroin hydrogels promotes angiogenesis. *Biomed Mater*. 2016;11:035009.
36. Yan S, Zhang Q, Wang J, et al. Silk fibroin/chondroitin sulfate/ hyaluronic acid ternary scaffolds for dermal tissue reconstruction. *Acta Biomater*. 2013;9:6771–6782.
37. Kaneko H, Dridi S, Tarallo V, et al. DICER1 deficit induces Alu RNA toxicity in age-related macular degeneration. *Nature*. 2011;471:325–330.
38. Carido M, Zhu Y, Postel K, et al. Characterization of a mouse model with complete RPE loss and its use for RPE cell transplantation. *Invest Ophthalmol Vis Sci*. 2014;55:5431–5444.
39. Stanzel BV, Liu Z, Somboonthanakij S, et al. Human RPE stem cells grown into polarized RPE monolayers on a polyester matrix are maintained after grafting into rabbit subretinal space. *Stem Cell Reports*. 2014;2:64–77.
40. Sugita S, Iwasaki Y, Makabe K, et al. Successful transplantation of retinal pigment epithelial cells from MHC homozygote iPSCs in MHC-matched models. *Stem Cell Reports*. 2016;7: 635–648.

Investigative Ophthalmology & Visual Science